Neural Network-Based Predefined-Time Robust Control for Quadrotors with Actuator Faults

Sanjeev Ranjan* and Kiran Kumari

***Abstract*—This paper addresses the predefined-time attitude and altitude tracking control problem of quadrotors subject to actuator faults, external disturbances, and model uncertainties. To address the discontinuity in controller and predefined-time convergence, a novel smooth arctan-based predefined-time sliding surface is introduced, replacing the existing piecewise-continuous function. The proposed controller ensures that the quadrotor's trajectory converges to the reference trajectory within the predefined time frame, irrespective of the initial system states. Furthermore, a radial basis function neural network (RBFNN) is implemented to approximate the uncertain components of the quadrotor system, thereby improving its stability. Additionally, an adaptive anti-fault compensation law is designed to counteract actuator faults while ensuring improved tracking performance. The stability of the predefined-time sliding-mode fault-tolerant control (FTC) is analyzed using the Lyapunov stability theorem. Finally, the efficacy of the proposed controller is demonstrated through an extensive simulation study that compares it with existing control methods.**

Keywords: **Quadrotors, predefined-time stability, fault-tolerant control, RBFNN, arctan function, Lyapunov stability.**

I. INTRODUCTION

In recent years, the application of unmanned aerial vehicles (UAVs), such as quadrotors, has experienced exponential growth, and UAVs are crucial in defense sectors, traffic inspection, surveillance, agriculture, and industrial applications. However, the underactuated and nonlinear dynamics of the quadrotor make it challenging to design a suitable controller for trajectory tracking. Additionally, due to motor malfunction or actuator degradation, an actuator fault may occur, degrading performance and even damaging the system. These actuator faults, combined with external disturbances, may cause critical missions or important tasks to fail. Therefore, the operational performance of UAVs in complex and hazardous environments is crucial for achieving the desired objective [1]. Furthermore, actuator faults and unknown external disturbances complicate the system's stability. Consequently, various control design techniques have been developed to improve trajectory tracking performance and stabilize the quadrotor, addressing actuator faults, external disturbances, and model uncertainties [2].

To address the above-cited challenges, a wide range of control techniques, including PID, backstepping, linear quadratic regulator, and nonlinear adaptive control, have been employed for quadrotor systems [3]. However, under external disturbances and model uncertainties, the performance of these control techniques degrades. Therefore, to enhance the performance, a robust control technique, namely sliding mode control (SMC), is implemented in [4]. SMC is one of the robust control techniques that helps mitigate the effect of unknown disturbances. To further enhance performance and convergence speed, different sliding surface-based control methods, including integral sliding mode, terminal sliding mode, and fast terminal sliding mode, have been developed [5]. However, these controllers suffer from either discontinuity or singularity. To overcome singularity, a nonsingular terminal sliding mode controller is designed in [6]. These control strategies exhibit finite-time convergence, and the stabilization time depends on the initial condition of the states. To relax this dependence, a fixed-time control design has been developed in [7]. Although existing fixed-time controllers can achieve the system's state convergence within the desired time by appropriately assigning control parameters, achieving convergence at an arbitrary predefined time set by the designer in advance is challenging. Moreover, establishing a direct relationship between tuning gains and the fixed stabilization time is not straightforward [8].

To overcome the limitations of finite and fixed-time design, prescribed-time controllers have been developed in [9]. Prescribed-time stability enables the designer to define the upper bound of convergence in advance, without relying on the initial conditions of the state parameters. A free-will arbitrary time control, which allows convergence in the prescribed time, is explored in [10]. However, the prescribed-time control strategy requires higher control effort during convergence [11]. Additionally, the prescribed time is usually an upper bound on the convergence time and is a conservative estimate [12].

Therefore, to address the limitations and challenges posed by prescribed-time design, a predefined-time control (PDC) strategy is developed, in which the prescribed-time stability coincides with the fixed-time stability and the true settling time is considered. Therefore, to handle actuator faults and external disturbances, and to ensure predefined-time stability, a nonsingular predefined-time fault-tolerant control (NPFTC) strategy is proposed in this paper. The contributions of the presented work are summarized as follows.

1) A novel nonsingular predefined-time sliding mode controller with a smooth arctan-based sliding manifold is designed for attitude and altitude tracking of a quadrotor, ensuring predefined-time stability with faster response. The settling time of the controller can be chosen in advance and is independent of the initial state conditions.
2) An anti-fault compensatory adaptive law is designed to counteract time-varying actuator faults and ensure minimal deflection from the reference path while tracking.
3) A RBFNN algorithm is implemented to approximate the

*Sanjeev Ranjan and Kiran Kumari are with the Department of Electrical Engineering, Indian Institute of Science, Bengaluru, Karnataka-560012, India. Email ID: {sanjeevr1, kirank}@iisc.ac.in. *ORCID: 0009-0004-0873-7047 .

uncertain part of the system, including model uncertainty and unknown external disturbances.

4) Lyapunov stability analysis is provided for the system with the RBFNN algorithm and adaptive law.

The subsequent sections are divided as follows. Section II describes the modeling of the quadrotor and preliminaries. Section III presents the proposed PDC design with adaptive law and NN. The simulation study is presented in Section IV. Lastly, Section V outlines the conclusion.

Notations: $\|\cdot\|$ is the Euclidean norm, $\exp(\cdot)$ denotes the exponential function, $\mathrm{sgn}(\cdot)$ represents the signum function, and $\mathrm{atan}(x)$ denotes $\arctan(x)$ or $\tan^{-1}(x)$ function.

II. Model Description and Preliminaries

A. Model Description

This section presents a dynamic model of the quadrotor system, defined in the body frame relative to the fixed reference frame. Attitude motions, such as roll, pitch, yaw, and vertical movement, can be obtained by adjusting the motor speed. The enhanced maneuverability and stability of the UAV result from the coordinated operation of all four motors. The model of the quadrotor derived through the Newton-Euler formulation is obtained as follows [13]

$$\begin{aligned}\ddot{z} &= \frac{u_1}{m}\Big(\cos\phi\cos\theta\Big) - g - \frac{k_t\dot{z}}{m} + d_1\\ \ddot{\phi} &= \frac{1}{I_x}\Big(\dot{\theta}\dot{\psi}(I_y - I_z) + \dot{\theta}I_r\Omega_t - k_r\dot{\phi} + u_2\Big) + d_2\\ \ddot{\theta} &= \frac{1}{I_y}\Big(\dot{\phi}\dot{\psi}(I_z - I_x) + \dot{\phi}I_r\Omega_t - k_r\dot{\theta} + u_3\Big) + d_3\\ \ddot{\psi} &= \frac{1}{I_z}\Big(\dot{\phi}\dot{\theta}(I_x - I_y) - k_r\dot{\psi} + u_4\Big) + d_4\end{aligned} \tag{1}$$

where $\Omega_t = -\Omega_1 + \Omega_2 - \Omega_3 + \Omega_4$ is the net residual rotor angular speed; I_x, I_y, and I_z are the moment of inertia along the x, y, and z axis, respectively; I_r is the rotor inertia, g is the gravitational constant, m is the total mass of the UAV; k_t and k_r are the translational and rotational drag coefficients, respectively, $d_i, (i = 1, \cdots, 4)$ are the unknown external disturbances. Coordinate z represents the altitude, and ϕ, θ, and ψ denote the angular positions, namely roll, pitch, and yaw angles, respectively. The control inputs produced by the rotation of four motors are expressed by

$$\begin{bmatrix}u_1\\u_2\\u_3\\u_4\end{bmatrix} = \begin{bmatrix}b_T(\Omega_1^2+\Omega_2^2+\Omega_3^2+\Omega_4^2)\\ b_Tl(\Omega_4^2-\Omega_2^2)\\ b_Tl(\Omega_1^2-\Omega_3^2)\\ c_D(-\Omega_1^2+\Omega_2^2-\Omega_3^2+\Omega_4^2)\end{bmatrix} \tag{2}$$

where $u_i, (i = 1, 2, 3, 4)$ are the control inputs produced by the four rotors, Ω_i are the rotational speeds of the i^{th} motor, b_T denotes the thrust coefficient, c_D is the ratio between the drag and thrust coefficient of the rotor, and l is the arm length.

Consider the state vector $x = [z\ \dot{z}\ \phi\ \dot{\phi}\ \theta\ \dot{\theta}\ \psi\ \dot{\psi}]^\top$. The quadrotor model in (1), considering the parametric uncertainty, can be expressed in the following nonlinear affine form

$$\dot{x}_{2i-1} = x_{2i}, \quad \dot{x}_{2i} = f_i(x) + \delta f_i(x) + b_iu_i + d_i \tag{3}$$

for $i = 1, 2, 3, 4$ where

$$f_i(x) = \begin{bmatrix}-g - \frac{k_tx_2}{m}\\ x_6x_8(I_y - I_z)/I_x + x_6(I_r/I_x)\Omega_t - (k_r/I_x)x_4\\ x_4x_8(I_z - I_x)/I_y + x_4(I_r/I_y)\Omega_t - (k_r/I_y)x_6\\ x_4x_6(I_x - I_y)/I_z - (k_r/I_z)x_8\end{bmatrix},$$

$b_i = \mathrm{diag}(\frac{\cos x_3 \cos x_5}{m}, \frac{1}{I_x}, \frac{1}{I_y}, \frac{1}{I_z})$ and $\delta f_i(x)$ is model uncertainty due to change in inertial moments and drag resistance.

Assumption 1: The unknown external disturbances d_i and model uncertainties δf_i are bounded such that $|d_i| \leq \overline{D}$, and $|\delta f_i| \leq \overline{F}$, where $\overline{D} > 0$, $\overline{F} > 0$ are scalars.

B. Actuator Fault Model

Consider the loss of effectiveness (LOE) actuator fault occurring in the control input u_i of the quadrotor system, which is related by the following relation

$$u_i^f = \sigma_iu_i + \xi_{i_b} \tag{4}$$

where u_i^f is the control input affected with faults, $\sigma_i \in (0, 1]$ denotes actuator control effectiveness factor, ξ_{i_b} is the additive bias fault.

Remark 1: For $\sigma_i = 1$, the actuator is healthy; whereas $0 < \sigma_i < 1$ indicates partial actuator failure.

Assumption 2: The additive bias fault ξ_{i_b} is bounded such that $|\xi_{i_b}| \leq \overline{\xi}$, where $\overline{\xi} > 0$ is a scalar.

After injecting the actuator fault (4), system (3) can be rewritten as

$$\dot{x}_{2i-1} = x_{2i}, \quad \dot{x}_{2i} = f_i(x) + \delta f_i(x) + b_iu_i^f + d_i. \tag{5}$$

For the convenience of controller design, the nonlinear model (5) can be represented as

$$\dot{x}_{2i-1} = x_{2i}, \quad \dot{x}_{2i} = f_i(x) + b_iu_i + \Phi_i(x, u) + \Delta_i \tag{6}$$

where $\Phi_i(x, u) = b_i\sigma_iu_i + b_i\xi_{i_b} - b_iu_i$ is the lumped actuator fault term, and $\Delta_i = \delta f_i(x) + d_i$ denotes the lumped uncertainty term of the system containing external disturbances.

Assumption 3: The lumped fault term Φ_i and lumped model uncertainty term Δ_i satisfies $|\Phi_i| \leq \overline{\Phi}$, and $|\Delta_i| \leq \overline{\Delta}$, respectively, where $\overline{\Phi} > 0$, $\overline{\Delta} > 0$ are scalars.

Control objective: The objective is to design a predefined time-based nonsingular sliding mode FTC to ensure the trajectory tracking of the UAV within the prespecified time frame, addressing actuator faults and unknown disturbances.

C. Preliminaries

Definition 2.1: [13] *Predefined-time stability*: Consider the following nonlinear system

$$\dot{x}(t) = f(t, x), \qquad x(0) = x_0, \tag{7}$$

where $x \in \mathbb{R}^n$ denotes the system state and $f : \mathbb{R}^+ \times \mathbb{R}^n \to \mathbb{R}^n$ is a continuous function. If, for any initial state $x(0)$, the solution satisfies $\|x(t)\| \leq \bar{x}$, $\forall t \geq T_c$, where $\bar{x}$ and T_c are positive scalars, then the equilibrium of system (7) is *predefined-time stable* (PDS), and the convergence time satisfies $T \leq T_c$, where T_c is regarded as the predefined time.

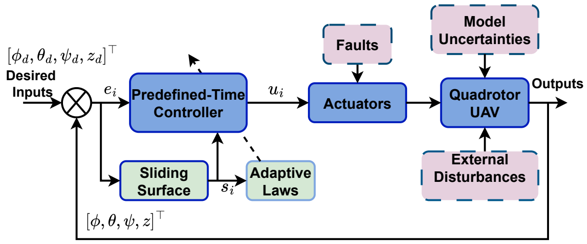

Fig. 1. The block diagram of the proposed control scheme.

Lemma 2.1: [14] Consider a first-order system as

$$\dot{x} = -\frac{\beta}{\gamma T_c(1-\eta)}\left(1+\gamma^2 x^2\right)|\mathrm{atan}(\gamma x)|^{2\eta-1}\,\mathrm{sgn}(\mathrm{atan}(\gamma x)), \tag{8}$$

where $\frac{1}{2} < \eta < 1$, $\gamma > 0$, $\beta \geq \frac{1}{2}\left(\frac{\pi^2}{4}\right)^{1-\eta}$, and $T_c > 0$ are design parameters. Then the system (8) is predefined-time stable, and the state $x(t)$ converges to zero before T_c. The convergence time is given by $T = \frac{T_c}{2\beta} V_1\big(x(0)\big)^{1-\eta} \leq \frac{T_c}{2\beta}\left(\frac{\pi^2}{4}\right)^{1-\eta}$, where $V_1(x) = \mathrm{atan}(\gamma x)^2$.

Lemma 2.2: [15] For any $z \in \mathbb{R}$ and $\varpi > 0$, the following inequality holds:

$$0 \leq |z| - z\,\tanh\Big(\frac{z}{\varpi}\Big) \leq 0.2785\,\varpi \tag{9}$$

Lemma 2.3: For the uncertain system $\dot{x} = f(t, x, d)$ if there exists a positive definite Lyapunov function $V(x)$ satisfying $\dot{V}(x) \leq \frac{-2\beta}{T_c(1-\eta)} V(x)^\eta + \Sigma$, where $0 < \Sigma < \infty$, β, and η are same as Lemma 2.1. Then the system's trajectory is practically predefined time stable with the convergence region $\left\{\lim_{t\to T_c'} x \mid V(x) \leq \left(\frac{T_c\Sigma(1-\eta)}{2(1-\mu)\beta}\right)^{\frac{1}{\eta}}\right\}$ where T_c' denotes the settling time satisfying $T_c' < T_c/\mu$ with $0 < \mu < 1$.

Proof: Kindly refer to the Appendix. ■

III. Controller Design and Stability Analysis

This section presents a predefined-time nonsingular SMC design that introduces an arctan-based sliding surface. The proposed closed-loop system architecture is presented in Fig. 1. The predefined-time sliding variable is designed as

$$s_i = \mathrm{atan}\left(\gamma_{1i} e_i\right) + \left(|\Lambda_i|\right)^{\frac{1}{2\eta_{1i}-1}}\mathrm{sgn}(\Lambda_i), \tag{10}$$

with

$$\Lambda_i = \frac{\gamma_{1i} T_{c1}(1-\eta_{1i})\,\dot{e}_i}{\beta_{1i}\left(1+\gamma_{1i}^2 e_i^2\right)}, \qquad i = 1, 2, 3, 4 \tag{11}$$

where $\frac{1}{2} < \eta_{1i} < 1$, $T_{c1} > 0$, $\gamma_{1i} > 0$, and $\beta_{1i} \geq 0.5\left(0.75\pi^2\right)^{1-\eta_{1i}}$ are all design parameters. Also, $e_i = x_i - x_{id}$ denotes the tracking error, where x_i is the actual state, and x_{id} is the desired state, T_{c1} is the predefined time required for the tracking error to converge to zero. The sliding manifold corresponding to the proposed sliding variable (10) is smooth and continuous.

Based on this sliding variable, the control input of the system can be computed as

$$\begin{aligned} u_i = &\frac{1}{b_i}\big(\ddot{x}_{i_d} - f_i(x) - \Phi_i - \Delta_i - G_{1i} + G_{2i} \\ &+ (G_{3i} G_{4i} G_{5i} G_{6i})\big) \end{aligned} \tag{12}$$

where $G_{1i} = -\frac{2\gamma_{1i}^2 e_i \dot{e}_i^2}{\left(1+\gamma_{1i}^2 e_i^2\right)^2}$;
$G_{2i} = \left(\frac{\beta_{1i}^2(2\eta_{1i}-1)}{\gamma_{1i}^2 T_{c1}^2(1-\eta_{1i}^2)}\right)\left(1+\gamma_{1i}^2 e_i^2\right)\left(\frac{T_{c1}(1-\eta_{1i})\,\dot{e}_i}{\beta_{1i}\left(1+\gamma_{1i}^2 e_i^2\right)}\right)^{\frac{4\eta_{1i}-3}{2\eta_{1i}-1}}$
$\mathrm{sgn}\left(\frac{T_{c1}(1-\eta_{1i})\,\dot{e}_i}{\beta_{1i}\left(1+\gamma_{1i}^2 e_i^2\right)}\right)$; $G_{3i} = -\left(\frac{T_{c1}(1-\eta_{1i})}{\beta_{1i}}\right)^{\frac{2\eta_{1i}-2}{2\eta_{1i}-1}}$,
$G_{4i} = \left(1+\gamma_{1i}^2 e_i^2\right)^{\frac{1}{2\eta_{1i}-1}}\ \Xi_\varrho\left(|\dot{e}_i|^{\frac{2-2\eta_{1i}}{2\eta_{1i}-1}}\right)$;
$G_{5i} = \frac{\beta_{1i}\beta_{2i}(2\eta_{1i}-1)(1+\gamma_{2i}^2 s_i^2)}{T_{c1}T_{c2}\gamma_{2i}(1-\eta_{1i})(1-\eta_{2i})}$;
$G_{6i} = |\mathrm{atan}(\gamma_{2i} s_i)|^{2\eta_{2i}-1}\,\mathrm{sgn}(\mathrm{atan}(\gamma_{2i} s_i))$ such that the following condition holds

$$\Xi_\varrho\left(|\dot{e}_i|^{\frac{2-2\eta_{1i}}{2\eta_{1i}-1}}\right) = \begin{cases} \sin\left(\dfrac{\pi}{2\varrho}\ |\dot{e}_i|^{\frac{2-2\eta_{1i}}{2\eta_{1i}-1}}\right), & |\dot{e}_i|^{\frac{2-2\eta_{1i}}{2\eta_{1i}-1}} \leq \varrho, \\ 1, & \text{otherwise.} \end{cases} \tag{13}$$

Here $0 < \eta_{2i} < 1$, $\varrho > 0$ is a sufficiently small scalar, $T_{c2} > 0$ is a predetermined time for the system state to reach the manifold s_i from the initial state, $\gamma_{2i} > 0$, and $\beta_{2i} \geq 0.5\left(0.75\pi^2\right)^{1-\eta_{2i}}$ are all control design parameters.

A. RBFNN Algorithm for Model Approximation

RBFNNs can approximate unknown continuous functions. It plays a key role in compensating for nonlinearities and in parameter estimation. Consider the lumped uncertain term Δ_i in (6) to approximate through the RBFNN algorithm [13]

$$\Delta_i = W_i^{*\top} H_i(z_i) + \varepsilon_i \tag{14}$$

where $z_i = [e_i\ \dot{e}_i]^\top$ is the input variable of NN, $W_i^* \in \mathbb{R}^n$ is the ideal RBFNN weight vector, ε_i is the NN approximation error which is bounded, i.e., $|\varepsilon_i| \leq \bar{\varepsilon}$ for $\bar{\varepsilon} > 0$, $H_i(z_i) = [H_{i1}\ H_{i2}\ \cdots\ H_{in}]^\top \in \mathbb{R}^n$ is the basis vector of the NN, and n denote the number of neuron nodes. The basis function is selected as

$$H_{ij}(z_i) = \exp\left(\frac{-\|z_i - c_{ij}\|^2}{\zeta_{ij}^2}\right), \quad \text{for } j = 1, \cdots, n \tag{15}$$

where $c_{ij} = [c_{i1}\ c_{i2}\ \cdots\ c_{in}]^\top$ is the central parameter of Gaussian function, and ζ_{ij} is the width of RBF network. Also, note that $H_i(z_i)$ will be referred to as H_i in the remaining sections for simplicity. The NN-based adaptive parameter is constructed as

$$\dot{\hat{W}}_i = \Upsilon_{1i} H_i s_i \tag{16}$$

where $\Upsilon_{1i} > 0$ is a scalar, $\hat{W}$ is approximated weights and H_i is the RBFNN vector. Further, to counter the actuator fault, an anti-fault compensation adaptive law is constructed as

$$\dot{\hat{\Phi}}_i = \Upsilon_{2i} s_i \tanh\left(\frac{s_i}{\varpi_i}\right) - \kappa_i \hat{\Phi}_i \tag{17}$$

where Υ_{2i}, ϖ_i, and κ_i are adaptive design parameters, and all are positive constants. Finally, incorporating the adaptive laws (16) and (17), the control input (12) can be modified as

$$u_i = \frac{1}{b_i}\big(\ddot{x}_{i_d} - f_i(x) - \hat{\Phi}_i \tanh\Big(\frac{s_i}{\varpi_i}\Big) - \hat{W}_i^\top H_i - G_{1i} + G_{2i} + (G_{3i}G_{4i}G_{5i}G_{6i})\big). \tag{18}$$

B. Stability Analysis

Theorem 3.1: Consider the system (6) with a lumped fault and uncertainty term. The control input (18) with the help of the sliding variable (10), and adaptive laws (16)-(17) ensures the convergence of the states to the vicinity of the desired trajectory within the predefined time $T_c < T_{c1} + T_{c2}/\mu$.

Proof: Consider the Lyapunov function candidate as

$$\mathcal{V}_i = \operatorname{atan}(\gamma_{2i}s_i)^2 + \frac{1}{2\Upsilon_{1i}}\tilde{W}_i^\top \tilde{W}_i + \frac{1}{2\Upsilon_{2i}}\tilde{\Phi}_i^2 \tag{19}$$

where $\tilde{W} = W^* - \hat{W}$ is the approximated error, $\tilde{\Phi} = \Phi - \hat{\Phi}$ is the estimated error of the lumped fault term. Firstly, consider the time duration T_{c2} for the states to reach the sliding manifold s_i. Substituting control input (18) to compute derivative of sliding variable obtained as

$$\dot{s}_i = -\Xi_\varrho\left(|\dot{e}_i|^{\frac{2-2\eta_{1i}}{2\eta_{1i}-1}}\right)\left(\frac{\beta_{2i}(1+\gamma_{2i}^2 s_i^2)}{T_{c2}\gamma_{2i}(1-\eta_{2i})}|\operatorname{atan}(\gamma_{2i}s_i)|^{2\eta_{2i}-1} \operatorname{sgn}(\operatorname{atan}(\gamma_{2i}s_i))\right) \tag{20}$$

Taking the first derivative of (19) yields

$$\dot{\mathcal{V}}_i = -\Xi_\varrho\left(|\dot{e}_i|^{\frac{2-2\eta_{1i}}{2\eta_{1i}-1}}\right)\left(\frac{2\beta_{2i}|\operatorname{atan}(\gamma_{2i}s_i)|^{2\eta_{2i}}}{(T_{c2}(1-\eta_{2i}))}\right) + \tilde{W}_i^\top H_i s_i - \frac{\tilde{W}_i^\top \dot{\hat{W}}_i}{\Upsilon_{1i}} - \frac{\tilde{\Phi}_i\dot{\hat{\Phi}}_i}{\Upsilon_{2i}} \tag{21}$$

For the convenience of stability proof, further state space region is divided into the following two different regions [16]:

$$\begin{aligned}\mathfrak{S}_1 &= \left\{(e_i,\dot{e}_i)\ \middle|\ |\dot{e}_i|^{\frac{2-2\eta_{1i}}{2\eta_{1i}-1}} \geq \varrho\right\},\\ \mathfrak{S}_2 &= \left\{(e_i,\dot{e}_i)\ \middle|\ |\dot{e}_i|^{\frac{2-2\eta_{1i}}{2\eta_{1i}-1}} < \varrho\right\}.\end{aligned} \tag{22}$$

If the state error variables $\big(e_i, \dot{e}_i\big)$ belong to $\mathfrak{S}_1$, then $\Xi_\varrho(\cdot)$ function takes the value 1. Further, (21) can be simplified by employing Lemma 2.2 as

$$\begin{aligned}\dot{\mathcal{V}}_i \leq& -\frac{2\beta_{2i}}{T_{c2}(1-\eta_{2i})}\mathcal{V}_i^{\eta_{2i}} - \tilde{\Phi}_i s_i \tanh(s_i/\varpi_i) + (\kappa_i/\Upsilon_{2i}|\Phi_i|^2)\\ \leq& -\frac{2\beta_{2i}}{T_{c2}(1-\eta_2)}\mathcal{V}_i^{\eta_{2i}} + 0.2785\varpi_i\Phi_i + |s_i|\Phi_i + (\kappa_i/\Upsilon_{2i}|\Phi_i|^2)\\ =& -\frac{2\beta_{2i}}{T_{c2}(1-\eta_{2i})}\mathcal{V}_i^{\eta_{2i}} + \Sigma_i\end{aligned} \tag{23}$$

where $\Sigma_i = 0.2785\varpi_i\Phi_i + |s_i|\Phi_i + (\kappa_i/\Upsilon_{2i}|\Phi_i|^2)$. Therefore, based on Lemma 2.3, the system states will stay on the sliding surface $s_i = 0$ or enter the region $\mathfrak{S}_2$ within a prespecified time T_{c2}/μ. Consider the second region $\mathfrak{S}_2$ with $0 < \Xi_\varrho < 1$ when $\dot{e}_i \neq 0$. Then the sliding surface $s_i = 0$ remains an attractor. To complete the analysis, it remains to show that e_i is not an attractor except for $(e_i, \dot{e}_i) = (0, 0)$. In close proximity to the e_i-axis, it can be inferred that $\Xi_\varrho(|\dot{e}_i|^{\frac{2-2\eta_{1i}}{2\eta_{1i}-1}})\,|\dot{e}_i|^{\frac{2\eta_{1i}-2}{2\eta_{1i}-1}} \to 1$ as $\dot{e}_i \to 0$.
Thus, following relation can be obtained:

$$\ddot{e}_i = \left(\frac{T_{c1}(1-\eta_{1i})}{\beta_{1i}}\right)^{\frac{2\eta_{1i}-2}{2\eta_{1i}-1}} \frac{\beta_{1i}\beta_{2i}(2\eta_{1i}-1)\left(1+\gamma_{2i}^2 s_i^2\right)}{T_{c1}T_{c2}\gamma_{2i}(1-\eta_{1i})(1-\eta_{2i})} |\operatorname{atan}(\gamma_{2i}s_i)|^{2\eta_{2i}-1}\operatorname{sgn}(\operatorname{atan}(\gamma_{2i}s_i)) - \hat{\Phi}_i\tanh\Big(\frac{s_i}{\varpi_i}\Big) - \hat{W}_i^\top H_i. \tag{24}$$

From (24), it can be implied that $\ddot{e}_i < 0$ for $s_i > 0$ and $\ddot{e}_i > 0$ when $s_i < 0$. Therefore, $\ddot{e}_i$ will transgress $\mathfrak{S}_2$ into $\mathfrak{S}_1$ monotonically in a finite time [16].

Based on the above stability analysis, the sliding surface $s_i = 0$ is achieved from any initial states in the space before $T_{c2}/\mu + \epsilon(\varrho)$. When the states reach the switching function ($s_i = 0$), they converge to zero before T_{c1}. Thus, the total convergence time can be calculated as $T_{C1} + T_{C2}/\mu$. ∎

Remark 2: [16] Traveling time $\epsilon(\varrho)$ cannot be computed precisely as it becomes very small if the constant ϱ is chosen sufficiently small. Therefore, due to the conservativeness of estimating the convergence time T_{c2}, $\epsilon(\varrho)$ can be ignored.

Remark 3: In contrast to existing predefined-time SMC approaches that tend to converge slowly under small initial conditions, this paper proposes an arctan-based sliding surface with parameter $\gamma_i > 0$ to enhance convergence when $x_i(0)$ is small. Additionally, two adaptive laws are implemented to handle actuator faults and model uncertainty separately, thereby avoiding overestimation of control gain parameters, unlike the work in [17], [18], which does not consider actuator faults within the PDC framework.

IV. Simulation Results and Discussion

To demonstrate the effectiveness of the proposed NPFTC design with predefined-time convergence for altitude and attitude tracking of the quadrotor, simulation results are presented and compared with those of the nonsingular sliding mode PDC (NSMPDC) method in [19]. The quadrotor UAV model parameters are taken from [10]. The external disturbance values are considered as $[d_1\ d_2\ d_3\ d_4] = [2.5\sin(2\pi t),\ 2.5\cos(2\pi t),\ 2.8\sin(2\pi t),\ 3.2\cos(2\pi t)]$. The model uncertainty is considered as the varying inertial moments of the UAV, which is taken as $\delta f_{\phi,\theta,\psi} = \delta I_{x,y,z} = \operatorname{diag}(0.04, 0.05, -0.06)$ along with the air drag factors referred from [10], and $\delta f_z = \delta k_t = 0.18$. The predefined convergence time is set to $T_{c1} = 2$ sec, and $T_{c2} = 2$ sec. The NPFTC control gains are selected to achieve the desired performance. While selecting control parameters, trade-offs between the convergence rate and control input requirements should be maintained. Control design parameters are chosen as $\gamma_{1i} = 80, \gamma_{2i} = 30, \eta_{1i} = 0.85, \eta_{2i} = 0.85, \Upsilon_{1i} = 15, \Upsilon_{2i} =$

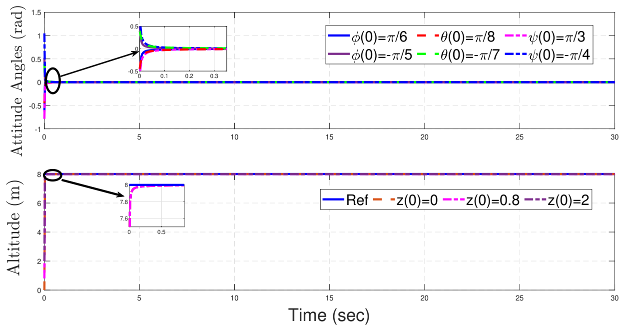

Fig. 2. Attitude and altitude tracking within $T_c < T_{c1} + T_{c2}/\mu$.

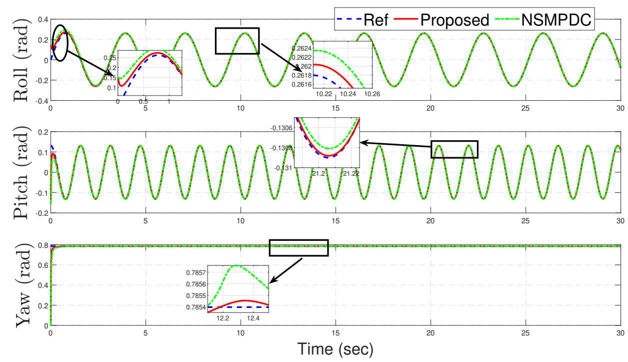

Fig. 3. Comparative result of attitude tracking with faults and disturbances.

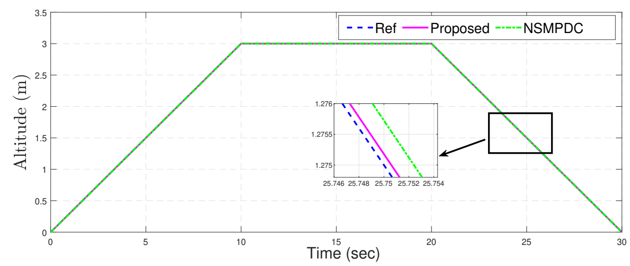

Fig. 4. Comparative result of altitude tracking with fault and disturbance.

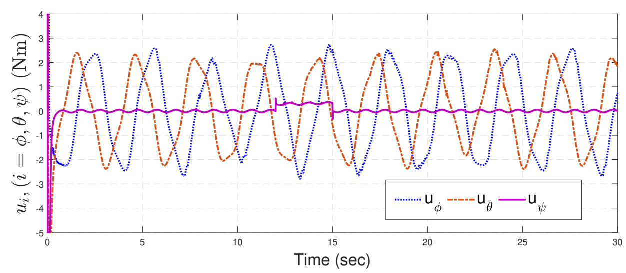

Fig. 5. Control inputs for attitude tracking.

$25, \kappa_i = 0.01, \varpi_i = 0.05$, and $\varrho = 0.001$. The RBFNN parameters c_i are placed evenly between $[-1.5, 1.5]$, $\zeta_i = 2$, and $n = 7$, $\hat{W}_i(0) = 0.1 * [1, 1, 1, 1, 1, 1, 1]$, and $\hat{\Phi}_i(0) = 0.02$.

Fig. 2 shows the convergence of the attitude and altitude states within the predefined time of 4 sec, for different initial conditions. This figure illustrates that the proposed controller ensures convergence within the predefined time, and independent of the initial state conditions. A time-varying actuator LOE factor is injected as $\sigma_i = [0.80 + 0.20\sin(0.5t), 0.75 + 0.20\cos(0.5t), 0.65 + 0.12\cos(t), 0.60 + 0.15\sin(t)]^\top$, and $\xi_{i_b} = [0.65, 0.45, 0.52, 0.55]^\top$ over different time intervals. For the tracking task, the initial conditions are considered as $[\phi(0), \theta(0), \psi(0), z(0)]^\top = [\pi/21, -\pi/20, 0, 0]^\top$. Fig. 3 presents the attitude tracking of the UAV system with external disturbances and actuator faults at different time intervals taken as u_ϕ^f for $t \in [8, 11]$ sec, u_θ^f for $t \in [21, 24]$ sec, and u_ψ^f over $t \in [12, 15]$ sec. These tracking results demonstrate the robustness of the proposed control scheme under time-varying fault scenarios with external disturbances. Subsequently, the tracking performance of the altitude having a time-varying reference is illustrated in Fig. 4 by introducing the LOE fault during time $t \in [25, 28]$ sec, to assess the robustness of the proposed FTC design. The control effort for attitude tracking of the quadrotor under faulty conditions is presented in Fig. 5. The performance indices of the proposed PDC with the existing (NSMPDC) method in [19] are summarized in Table I, including the convergence time, and integral time-weighted absolute error (ITAE) with error bound taken as $-0.01 \leq e_i \leq 0.01$, to further validate the effectiveness of the proposed method. These performance metrics indicate that the proposed NPFTC framework outperforms the existing method by achieving superior tracking accuracy and faster convergence, while effectively compensating for actuator faults, model uncertainties, and external disturbances.

TABLE I
PERFORMANCE INDICES OF DIFFERENT CONTROLLERS.

States	Schemes	**Convergence Time** (sec)	**ITAE** (rad · sec)
ϕ	Proposed	1.1548	0.07193
	NSMPDC	2.8756	0.1019
θ	Proposed	1.0113	0.08151
	NSMPDC	1.8653	0.1174
ψ	Proposed	0.9275	0.03104
	NSMPDC	1.4536	0.4366
z	Proposed	0.9275	0.2169
	NSMPDC	1.4536	1.1460

V. CONCLUSION

This work proposes an RBFNN-based predefined-time FTC strategy to address attitude and altitude tracking problems in the presence of actuator faults, model uncertainty, and external disturbances. The proposed NPFTC method introduces a novel arctan-based sliding surface for the quadrotor system, ensuring convergence within a predefined time and improved fault-tolerant capability. Moreover, two adaptive laws are incorporated within the proposed control law to counteract actuator faults and model uncertainty, independently, thereby avoiding overestimation of the gain parameters. The simulation studies confirm faster convergence and improved tracking accuracy in the presence of actuator faults and disturbances, compared with the conventional PDC method.

Appendix: Proof of Lemma 2.3

The inequality described in Lemma 2.3 can be rewritten in the following form

$$\dot{V}(x) \leq \frac{-2\mu\beta}{T_c(1-\eta)}V(x)^\eta + \left(\Sigma - \frac{2(1-\mu)\beta}{T_c(1-\eta)}V(x)^\eta\right) \quad (25)$$

From 25, it can be further proved that

$$\dot{V}(x) \leq \frac{-2\mu\beta}{T_c(1-\eta)}V(x)^\eta \quad (26)$$

if $\Sigma - \frac{2(1-\mu)\beta}{T_c(1-\eta)}V(x)^\eta \leq 0$. Further solving this can be simplified as $V(x)^\eta \geq \frac{T_c\Sigma(1-\eta)}{2(1-\mu)\beta}$.

Then, using the result of Lemma 2.3, it can be obtained and proved that the trajectory is practically predefined time stable, given by $\left\{\lim_{t\to T_c'} x \mid V(x) \leq \left(\frac{T_c\Sigma(1-\eta)}{2(1-\mu)\beta}\right)^{\frac{1}{\eta}}\right\}$. The following method is used to obtain the settling time of the uncertain quadrotor system.

From (26), the following inequality holds outside the set:

$$\dot{V}(x) \leq -\frac{2\mu\beta}{T_c(1-\eta)}V(x)^\eta, \qquad \forall\, V(x) > V_f \quad (27)$$

where $V_f = \left(\frac{T_c\Sigma(1-\eta)}{2(1-\mu)\beta}\right)^{\frac{1}{\eta}}$. Separating variables yields

$$V(x)^{-\eta}dV(x) \leq -\frac{2\mu\beta}{T_c(1-\eta)}dt. \quad (28)$$

Integrating both sides from $V(x(0))$ to V_f, and from 0 to T_c', results in

$$T_c' \leq \frac{T_c}{2\mu\beta}\left(V(x(0))^{1-\eta} - V_f^{1-\eta}\right). \quad (29)$$

Using the boundedness property of the arctan function $|\operatorname{atan}(x)| \leq \frac{\pi}{2}$, the Lyapunov function satisfies

$$V(x) = \operatorname{atan}(x)^2 + \delta_M \leq \frac{\pi^2}{4} + \delta_M \quad (30)$$

where $\delta_M = \frac{1}{2\Upsilon_{1i}}\tilde{W}_i^\top(0)\tilde{W}_i(0) + \frac{1}{2\Upsilon_{2i}}\tilde{\Phi}_i^2(0)$. Therefore, the settling time can be upper-bounded as

$$T_c' \leq \frac{T_c}{2\mu\beta}\left[\left(\frac{\pi^2}{4} + \delta_M\right)^{1-\eta} - V_f^{1-\eta}\right]. \quad (31)$$

Selecting $\beta = \frac{1}{2}\left(\frac{\pi^2}{4} + \delta_M\right)^{1-\eta}$, yields

$$T_c' \leq \frac{T_c}{\mu}\left[1 - \frac{V_f^{1-\eta}}{\left(\frac{\pi^2}{4} + \delta_M\right)^{1-\eta}}\right]. \quad (32)$$

Since $V_f > 0$, and $(\frac{\pi^2}{4} + \delta_M) > 0$, it follows that $T_c' < \frac{T_c}{\mu}$, if following condition holds $\left(\frac{V_f}{\frac{\pi^2}{4}+\delta_M)}\right)^{1-\eta} < 1$. This inequality can be ensured by appropriate selection of control parameters and initial values $\tilde{W}_i(0)$ and $\tilde{\Phi}_i^2(0)$. Hence, the uncertain system trajectories converge to the residual compact set $\Omega_V = \left\{x : V(x) \leq \left(\frac{T_c\Sigma(1-\eta)}{2(1-\mu)\beta}\right)^{\frac{1}{\eta}}\right\}$ within the predefined time T_c/μ, thereby guaranteeing practical predefined-time stability.

Remark 4: The primary contribution of the proposed Lemma 2.3 lies in extending the stability analysis established in the existing work presented in Lemma 2.1.

References

[1] Y. Wang, B. Jiang, Z.-G. Wu, S. Xie, and Y. Peng, "Adaptive sliding mode fault-tolerant fuzzy tracking control with application to unmanned marine vehicles," *IEEE Transactions on Systems, Man, and Cybernetics: Systems*, vol. 51, no. 11, pp. 6691–6700, 2020.

[2] H. Mo and G. Farid, "Nonlinear and adaptive intelligent control techniques for quadrotor uav–a survey," *Asian Journal of Control*, vol. 21, no. 2, pp. 989–1008, 2019.

[3] H. Shraim, A. Awada, and R. Youness, "A survey on quadrotors: Configurations, modeling and identification, control, collision avoidance, fault diagnosis and tolerant control," *IEEE Aerospace and Electronic Systems Magazine*, vol. 33, no. 7, pp. 14–33, 2018.

[4] H. Razmi and S. Afshinfar, "Neural network-based adaptive sliding mode control design for position and attitude control of a quadrotor uav," *Aerospace Science and technology*, vol. 91, pp. 12–27, 2019.

[5] B. Gao, Y.-J. Liu, and L. Liu, "Adaptive neural fault-tolerant control of a quadrotor uav via fast terminal sliding mode," *Aerospace Science and Technology*, p. 107818, 2022.

[6] N. P. Nguyen, H. Oh, and J. Moon, "Continuous nonsingular terminal sliding-mode control with integral-type sliding surface for disturbed systems: Application to attitude control for quadrotor uavs under external disturbances," *IEEE Transactions on Aerospace and Electronic Systems*, vol. 58, no. 6, pp. 5635–5660, 2022.

[7] S. Zhou, K. Guo, X. Yu, L. Guo, and L. Xie, "Fixed-time observer based safety control for a quadrotor uav," *IEEE Transactions on Aerospace and Electronic Systems*, vol. 57, no. 5, pp. 2815–2825, 2021.

[8] Y. Zhang, S. Tang, and J. Guo, "Adaptive terminal angle constraint interception against maneuvering targets with fast fixed-time convergence," *International Journal of Robust and Nonlinear Control*, vol. 28, no. 8, pp. 2996–3014, 2018.

[9] A. K. Pal, S. Kamal, S. K. Nagar, B. Bandyopadhyay, and L. Fridman, "Design of controllers with arbitrary convergence time," *Automatica*, vol. 112, p. 108710, 2020.

[10] S. Ranjan and S. Majhi, "Fixed-time observer-based adaptive free-will arbitrary time intelligent fault-tolerant control for an autonomous quadrotor," *International Journal of Systems Science*, pp. 1–24, 2025.

[11] A. K. Pal, S. Kamal, X. Yu, S. K. Nagar, and B. Bandyopadhyay, "Free-will arbitrary time terminal sliding mode control," *IEEE Transactions on Circuits and Systems II: Express Briefs*, vol. 69, no. 7, pp. 3189–3193, 2022.

[12] J. D. Sánchez-Torres, E. N. Sanchez, and A. G. Loukianov, "Predefined-time stability of dynamical systems with sliding modes," in *2015 American control conference (ACC)*. IEEE, 2015, pp. 5842–5846.

[13] S. Ranjan and S. Majhi, "Adaptive neural predefined-time attitude control of an uncertain quadrotor uav with actuator fault," *IEEE Transactions on Circuits and Systems II: Express Briefs*, 2024.

[14] N. Xuan-Mung, M. Golestani, S. Mobayen, and H. Kong, "Predefined-time disturbance observer-based attitude tracking control for spacecraft: A solution for arbitrary disturbances," *IEEE Transactions on Industrial Electronics*, 2025.

[15] M. M. Polycarpou, "Stable adaptive neural control scheme for nonlinear systems," *IEEE Transactions on Automatic control*, vol. 41, no. 3, pp. 447–451, 2002.

[16] Z. Zuo, "Nonsingular fixed-time consensus tracking for second-order multi-agent networks," *Automatica*, vol. 54, pp. 305–309, 2015.

[17] J. F. Trentin and D. A. Santos, "Predefined-time sliding mode attitude control for a quadrotor aerial vehicle," in *16th International Workshop on Variable Structure Systems (VSS)*, 2022, pp. 59–64.

[18] C.-D. Liang, M.-F. Ge, Z.-W. Liu, Y.-W. Wang, and H. R. Karimi, "Predefined-time terminal sliding mode control of robot manipulators," *arXiv preprint arXiv:2001.04198*, 2020.

[19] Y. Ji, P. Li, Y. Lin, Y. Song, Q. Gao, and J. Liu, "Predefined time attitude control of aircraft based on predefined time sliding mode control," *Proceedings of the Institution of Mechanical Engineers, Part I: Journal of Systems and Control Engineering*, vol. 239, no. 2, pp. 247–259, 2025.